Discovery of New Delhi Metallo-β-Lactamase-1(NDM-1) Inhibitors From Natural Compounds: In Silico-Based Methods

Azhar Salari-jazi
Isfahan University of Medical Sciences https://orcid.org/0000-0001-6591-1815
Karim Mahnam
Shahrekord University https://orcid.org/0000-0002-9906-4957
Parisa Sadeghi
Isfahan University of Medical Sciences https://orcid.org/0000-0002-4405-3388
Mohammad Sadegh Damavandi
Isfahan University of Medical Sciences https://orcid.org/0000-0002-2582-8838
Jamshid Faghri (damavand.mohammad@yahoo.com)
Isfahan University of Medical Sciences https://orcid.org/0000-0001-7500-168X

Research article

Keywords: New Delhi metallo-β-lactamase, Virtual screening, docking, Molecular dynamics simulation, 3D conformational alignment

DOI: https://doi.org/10.21203/rs.3.rs-50195/v1

Abstract

New Delhi metallo-β-lactamase variants and different types of metallo-β-lactamases have attracted enormous consideration for hydrolyzing almost all β-lactam antibiotics, which leads to multi drug resistance bacteria. Metallo-β-lactamases genes have disseminated in hospitals and all parts of the world and became a public health concern. There is no inhibitor for new Delhi metallo-β-lactamase-1 and other metallo-β-lactamases classes, so metallo-β-lactamases inhibitor drugs became an urgent need. In this study, multi-steps virtual screening was done over the NPASS database with 35032 natural compounds.

At first Captopril was extracted from 4EXS PDB code and use as a template for the first structural screening and 500 compounds obtained as hit compounds by molecular docking. Then the best ligand, i.e. NPC120633 was used as templet and 800 similar compounds were obtained. As a final point, ten compounds i.e. NPC171932, NPC100251, NPC18185, NPC98583, NPC112380, NPC471403, NPC471404, NPC472454, NPC473010 and NPC300657 had proper docking scores, and a 50 ns molecular dynamics simulation was performed for calculation binding free energy of each compound with new Delhi metallo-β-lactamase. 3D conformational alignment and protein sequence alignment of all new Delhi metallo-β-lactamase variants and all types of metallo-β-lactamases were done. Then the conserved and crucial residues in the catalytic activity of metallo-β-lactamases were detected. These residues had similar 3D coordinates in the 3D conformational alignment. So it is possible that all types of metallo-β-lactamases can inhibit by these ten compounds. Therefore, these compounds were proper to mostly inhibit all new Delhi metallo-β-lactamase and metallo-β-lactamases in experimental studies.

Introduction

Multi-drug resistance has become a significant threat to global health, and it appears that discovery of new class antibiotics is in an uttermost need for humankind [1]. Globally, beta-lactam antibiotics have been extensively prescribed to treat bacterial infections [2]. The considerable rise of antibiotic resistance in bacteria emanates from excessive use of beta-lactam antibiotics [2]. Beta-lactamases in bacteria are the most common mechanism to hydrolyze beta-lactam antibiotics and their resistance [3, 4].

β-lactamase enzymes are a bacterial defense mechanism to hydrolyze amide bond in beta-lactam antibiotics that inactivate them. According to the Ambler classification, beta-lactamases are divided into four classes (A, B, C, and D) consisting of two major families: Serine-β-lactamases (SBLs) and Metallo-β-lactamases (MBLs) [3, 4].

SBLs (A, C, and D Ambler's class) are serine hydrolases, while MBLs (B class) perform zinc ion in the active site as metallo -enzyme. Metallo-β-lactamases, owing to their broad-spectrum activities in the hydrolase of β-lactam antibiotics, are a considerable danger for human health.

MBLs are divided into subclasses B1, B2, and B3, and subclass B1 has the most clinical relevance and most commonly emergence among MBLs enzymes. This class has been found in Enterobacteriaceae members, and the enzyme members of this class have two ion zinc in the active site. Some enzymes of

subclass B1 consisting of VIM (Verona integron-borne metallo-β-lactamase), IMP (imipenemase), and NDM (New Delhi metallo-β-lactamase-1) have the highest frequency [4].

First time in 2009, New Delhi metallo-β-lactamase-1 (NDM-1) was identified in *Klebsiella pneumonia* from a clinical sample isolated from a tourist patient in New Delhi [5]. Further assessments showed that this enzyme had high resistance to all classes of beta-lactam antibiotics except monobactams [6]. After the NDM-1 first report, variants of this enzyme emerged in the world and it became a global concern [7]. Furthermore, most plasmids carrying the NDM-1 gene often associated with other resistance genes, such as sulfonamides, rifampin, chloramphenicol, quinolones, and macrolides [8, 9]. This property converts NDM-1 carrying bacteria to multi-drug resistant bacteria. Hence, NDM positive strains with these broad resistances to multiple drugs have grown a severe worldwide menace.

The worldwide distribution of NDM-1 has a considerable impact on treating different kinds of infections. Currently, there is no potent inhibitor against this enzyme; therefore, finding an inhibitor for it has become indispensable [10, 11]. Natural products (NPs) are a safe resource for human use and are suggested as a valuable source substitute for small molecule drugs. NPs are secondary metabolites derived from natural sources, e.g., micro-organisms, plants and animals, which have valuable and considerable biological activity [12–14]. These molecules have been selected within thousands of years to improve human health. In this study, the Natural Products Activity and Species Source (NPASSv1.0) database is used to screen natural compounds against NDM-1. Currently, the NPASS database consists of 35032 NPs from different species sources. Traditional chines medicine (TCM) plants and different kinds of NPs and plants are included in this database [15].

The present study aimed to target NDM-1 and found hotspot residues in all types of MBL. These residues can contribute to the better finding of the ligands in order to inhibit all MBLs.

Method

All steps of this study display in Fig. 1.

Protein and ligand preparation

High-resolution X-ray diffraction of NDM-1 structures include bound NDM-1 to the hydrolyzed ampicillin (PDB ID: 5ZGE) were downloaded from protein data bank (https://www.rcsb.org/pdb). 5ZGE consist of two NDM-1 molecules bound to the hydrolyzed ampicillin. Among two molecules, chain A was selected, and chain B omitted. NDM-1 enzyme contained 241 amino acids and two zinc ions, initiating from GLU 30 and terminating at ARG 271 position. Captopril was extracted from 4EXS PDB code and use as a template for the first structural screening in the infiniSee 1.3 software.

At first, all water molecules were deleted, hydrogen atoms added with the Discovery Studio software 2.5 (DS, Accelrys Inc, San Diego), and proteins prepared for the virtual screening and docking. Energy minimization was done with a simulation module of Discovery Studio via conjugating gradient method and CHARMm force field, until energy gradient fell below 0.1 calÅ^{-1} [16].

Selection of hit compound and Primary virtual screening

In the first structural screening, captopril was used as the template to find hit compound from the NPASS database through infiniSee 1.3 software. This database consisted of 35032 NPs from different species sources. In this step, 500 compounds were screened, minimized and docked (primary virtual screening) into NDM-1(5ZGE) by Autodock Vina module of the LigandScout.

Among the 500 compounds, NPC120633 had the best affinity of docking (in SeeSAR 10.0 software similar results obtained), so NPC120633 selected as the pattern for the second structural screening in infineSee 1.3 software.

Second structural screening

Second structural screening was performed to identify hit compounds from the NPASSv1.0 database (http://bidd2.nus.edu.sg/NPASS/) by infiniSee 1.3 software.

This structural screening was done over the NPASS database (similarity 75–100, based on the resemblance to NPC120633 obtained from the previous step) lead to 800 compounds. This collection was minimized by MMFF94 energy method in the LigandScout 4.3 to dock in the Autodock Vina module of the LigandScout [17, 18].

Molecular docking (secondary virtual screening)

Autodock Vina module of the LigandScout 4.3 was employed to dock all ligands to NDM-1, and SeeSAR 9.2 software performed to evaluate accuracy of docking result. At first, Autodock Vina was applied for the primary docking of the 800 ligand collection. The applied grid map was at 20 × 20 × 20 points for x, y and z dimensions with grid spacing of 1.0 Å. The coordinates of center grid box were placed at 0.772 Å, 51.827 Å, 106.874 Å for the x, y and z-axes, respectively. Default parameters for the Lamarckian genetic algorithm were applied and the numbers of run were on the 40 for profile docking (19).

The profiles of interactions among selected ligands and NDM-1 took through LigPlot and Discovery Studio Visualizer softwares [19, 16].

Finally, the best compounds which had the proper docking score in the Autodock Vina redocked to NDM-1 by Schrödinger suite software with standard precision (SP) docking and extra precision (XP) docking methods [20]. This redocking process lead to verification of position of ligands in active site of protein.

ADME/T Properties

The best compound which had proper docking score was selected for ADME/T properties calculation [20]. QIKPROP module of the Schrödinger suite was applied to calculate the ADME/T properties.

Molecular dynamic simulation

Ten selected NPs which achieved from redocking and had adequate docking score passed to this step.

The molecular dynamic simulations were used by AMBER18 package, and LEAP module performed to add hydrogen to atoms. AM1-BCC method of the Antechamber module was performed to produce NPs charge. The topology of macromolecules was generated via the leap module of AMBER tools with the AMBER99SB force field[21, 22][21, 22]. The generalized AMBER force field (GAFF2) in the Antechamber module of AMBER18 was applied to build the ligands topology. Then complexes were solvated in a truncated octahedral box of TIP3P water molecules with diameter of 10 Å. The boxes were neutralized by one Na^+ ion.

Two zinc ions in PDB structure were connected to NE2 of His 189, ND1 of His 122, NE2 His 120 and NE2 of His 250, OD2 of Asp 124, SG of Cys 208 via tleap module of Amber18.

For each system, sander module was used for energy minimization. Ten thousand cycles of minimization done to delete the bad steric interactions and to made better minimum energy via the conjugate gradients and steepest descent for all parts of the systems. Thereafter, the position restraints were performed at the constant volume (NVT) for 100 ps by a restraint force of 10 kcal/mol at the temperature of 100 K, and at constant pressure (NPT) for 100 ps by a restraint force of 1 kcal/mol at the temperature of 300 K.

Next, the system was equilibrated at NPT ensemble in density for 100 ps at pressure 1 atm and 300 K, while the restraint force was removed. This method led to equilibrate density for the system. Langevin dynamics were applied to control the temperature of systems.

Fifty nanosecond MD simulation with time step 2 fs in the final step was performed for each protein-ligand complex. CPPTRAJ of AMBER18 was used for analyze of MD simulations [23].

Binding energy and thermodynamic parameter calculation

Molecular Mechanics/Poisson-Boltzmann Surface Area (MM-PBSA) and Molecular Mechanics-Generalized Born Surface Area (MM-GBSA) are effective methods in Computer-Aided Drug Design (CADD) for calculation of the binding free energy. The binding free energy for each complex was calculated with MMPBSA.py script in AMBER18 package using below equation.

$$\Delta G_{binding}=G_{complex}-G_{protein}-G_{ligand}$$

Calculation of the binding free energy by MM-PBSA and MM-GBSA in the molecular dynamics simulations showed the accuracy of docking. The last ten ns of MD simulation trajectories were used to calculate the binding free energy [23].

3D conformational alignment and pharmacophore modeling

3D conformational alignment of the structures was done by the chimera software and simultaneously protein sequences alignments done on the structures by BLBD databases (Beta-Lactamase DataBase - Structure and Function; http://bldb.eu/). These sorts of calculations help to find some residues which may not conserve in the 2D alignment of the protein and analog residues among two types of enzymes.

Distances and angels among the amino acids of active sites calculated via the LigandScout software and pharmacophore modeling were done between representative kinds of MBLs. These data were compared. Three typical patterns of MBL classes (NDM1-BJP-Cph) docked with biapenem in autodock vina and post-docking processing done by LigPlot.

In fact, common pharmacophore and key amino acids in active site of all MBL classes and their subclasses were found by pharmacophore modeling, 3D conformational alignments, protein sequence alignments over eighty-six type of MBL from three subclass and their subtype (more than 700 subtypes), assessment of distances and angles between crucial amino acids. Comparison of these data showed common pharmacophore and key amino acids among all class of MBL was matchable. Finally, to confirm the efficacy of above data, biapenem was docked in the three classes of MBL. Docking processes showed key residues had involved in the docking and all three docking results had common pharmacophore

Results

The virtual screening

In the first structural screening, captopril is performed as the template to find the hit compound from the NPASS database via infiniSee 1.3 software. In this step, 500 compounds were screened. These compounds were minimized and docked to NDM-1 by Autodock Vina module of LigandScout 4.3. Among the 500 compounds, NPC120633 had the best binding affinity energy of -18.1 kcal/mol (in the SeeSAR 10.0 software similar results were obtained), so NPC120633 selected as the pattern for the second structural screening in the infineSee 1.3 software. The structure of captopril and NPC120633 were shown in Fig. 2.

The docking result

Eight hundred compounds were docked in second screening step via Autodock Vina and among them, ten compounds had the proper and higher affinity binding. Also in SeeSAR software a similar ranking of scores were obtained. The binding energy of ten selected NP obtained from Vina software, i.e NPC171932, NPC100251, NPC18185, NPC98583, NPC112380, NPC471403, NPC471404, NPC472454, NPC473010 and NPC300657 were − 24.3 kcal/mol, -22.9 kcal/mol, -22.8 kcal/mol, -22.2 kcal/mol, -22.80 kcal/mol, -21.8 kcal/mol, -22.3 kcal/mol, -22.7 kcal/mol, -21.3 kcal/mol and − 20.8 kcal/mol respectively. In the Schrödinger suite, these compounds had adequate sp- and xp-docking score (Table 1). The corresponding docking binding affinity k_b of all ligands were at the high level (Table 2). Binding affinity energy of Vina and XP and SP Glide score and hydrogen bonds and hydrophobic contacts were exhibited for all ligands with protein were mentioned in Fig. 1 and Table 1.

Table 1. The binding energy of Autodock Vina and Schrodinger suite of all NPs.

Complex	Structure	Glide XP Score kcal/mol	Glide E-Model	Glide SP-Score kcal/mol	autodock vina kcal/mol	TC	K_d (77^{-77})
NDMI-NPC18185	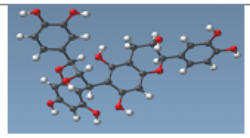	-10.00	-64.58	-7.51	-22.8	0.23	4.6×10^{16}
NDMI-NPC98583	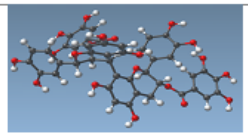	-7.78	-62.64	-7.15	-22.2	0.27	1.7×10^{16}
NDMI-NPC100251	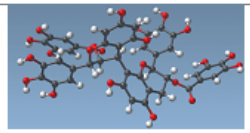	-13.95	-100.1	-8.32	-22	0.22	1.2×10^{16}
NDMI-NPC112380	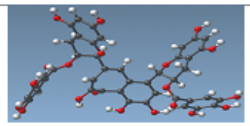	-12.76	-89.03	-8.59	-22.80	0.28	4.6×10^{16}
NDMI-NPC171932	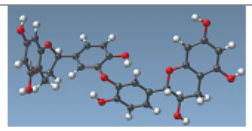	-8.395	-86.56	-8.12	-24.3	0.22	5.8×10^{17}
NDMI-NPC471403	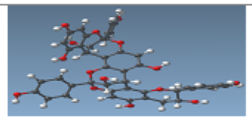	-9.036	-71.40	-7.07	-21.8	0.20	9.6×10^{15}
NDMI-NPC471404	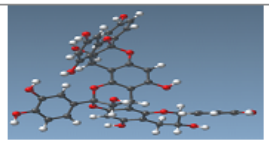	-8.561	-72.09	- 8.53	-22.3	0.20	2×10^{16}
NDMI-NPC472454	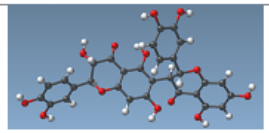	-10.06	-46.60	-7.37	-22.7	0.25	3.9×10^{16}
NDMI-NPC473010	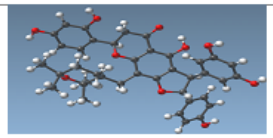	-7.01	-62.85	-7.11	-21.3	0.30	3.7×10^{15}
NDMI-NPC300657	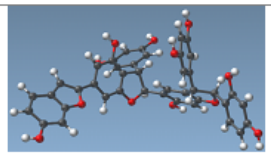	-10.068	-91.49	-8.10	-20.8	0.25	1.6×10^{15}

Hydrogen bonding and hydrophobic interactions of the complexes and distance between atoms ligands and protein were shown in Table 2.

Table 2
Hydrogen bonding and hydrophobic interactions of the complexes and distance between atoms ligands and protein

complex	Hydrogen bonds		Zinc interactions		Hydrophobic interaction	
	Residue	Distance (Å)	Zincs	Distance (Å)	Amino acids	Distance (Å)
NDM1-NPC18185	Asp212, Ser217, Ser251, His250, Asp124	2.21–3.13	Zinc303	2.58–3.15	His250, Ile35, Gly219, Asn220 ,Val73, Trp93, Gln23, His122, Asp124, Ser251, Lys211, Asp212, Ser217	3.30–4.30
NDM1-NPC98583	Gln23, Asp124, His250, Ser251, Thr134, Lys211	2.60–3.25	Zinc303	2.60–3.25	Ile35, Lys211, Gly36, Phe70, Ser217, Gly219, Lys211, His189, Asn220, Trp93, Met67, Gln23, Asp124, His122, His250, Ser251	3.42–4.02
NDM1-NPC100251	Ser217, Asp212, Ser251, His250,	2.13–3.16	Zinc302-Zinc303	2.21–2.77	Ser217, Gly219, Asn220, Phe70, His189, Gln123, Met67, Ile35, Ala215	3.4–4.40
NDM1-NPC112380	Ser217, Gly36, Ser251, His250, Lys211, Asn220	2.06–3.19	Zinc303	2.06	Asn220,Val73,Trp93, Gln23, Lue65, His189, Asp124, His250, Cys208, Lys211, Gly36, Ser251, Ser217, Ile35, Gly219	3.46–3.9
NDM1-NPC171932	His250, Ser251, Gly36, Lys211, Ser217	2.85–3.16			His250, Gly36, Ile35, Trp93, Lue65, Gln123, His122, Lys211, His189, Ser217, Gly219	2.88–4.4
NDM1-NPC471403	Asn220	3.28	Zinc302-Zinc303	2.54–2.87	Asn220, Cys208, Asp124, His189, Gln123, Lue65, Gly222, Lue221, Gly219, Ile35	3.8–5.6
NDM1-NPC471404	Asn220, Ser217	3.07–3.12	Zinc302-Zinc303	2.72–2.78	Asn220, Ser217, Ile35, Trp93, Asp124, His189, Lue65, Gln123, Gly222, Lue221, Gly219	3-4.69

complex	Hydrogen bonds		Zinc interactions		Hydrophobic interaction	
	Residue	Distance (Å)	Zincs	Distance (Å)	Amino acids	Distance (Å)
NDM1- NPC472454	Asp124, Ser251, Asp212, Ser217,	2.65–3.25	Zinc303	3.25	Ile35, Ser251, Lys211, Asp212, Ala215, Gly219, Phe70, Met67, Asn220 Gln123, His122, Trp93, Asp124	3.74–5.1
NDM1- NPC473010	Lys211, Gln123,	3-3.33	Zinc303	3.10	His250, Lys211, Gly219, Ile35, Val73, Met67, Lue65, Pro68, Gln123, His122, His189, Asp124, Asn220	3.36–4.69
NDM1- NPC300657	Asp124, Gln123, Lys211, Ser217	2.82–3.19	Zinc303	2.83	Asp124, Trp93, His250, Lue221, His189, Lys211, Lue221, Ser217, Phe70, Met67, Ile35, His122, Gln123	3.1–3.9

Hierarchical clustering of compounds placed in the Figure S1 (supplementary) and show that final compounds had good diversity. Tanimoto coefficient score of ten selected molecules were in the range of 0.2–0.3 in comparison to NPC120633 as reference molecule (Table 1)

Physio-chemical and ADME/T properties

Physio-chemical and the ADME/T properties of the ten docked NPs were calculated via ligandscout and QIKPROP of Schrödinger suite. Physio-chemical were indicated in the Table 3.

ADME/T properties consisted of the values for polarizability (QPpolrz), aqueous solubility (QPlogS), hexadecane/gas (QPlogPC16), water/gas (QPlogPw), octanol/water (QPlogPo/w), skin permeability (QPlogKp), and Khsa serum protein binding (QPlogKhsa) which have standard ranges as 13 to 70, -6 to 0.5, 4 to 18, 8 to 43, -2 to 6, -8.0 to -1.0, and 1.5 to 1.2, respectively [24]. The QIKPROP analysis exhibited values of QPpolrz, QPlogS, QPlogPC16, QPlogPoct, QPlogPw, QPlogPo/w, QPlogKp, and QPlog Khsa were in the standard range (Table 3).

Based on these analyses, the ADME/T properties of all ten compounds have in the standard limits for a potential candidate drug compound.

Table 3
ADME/T properties: Adsorption, Distribution, Metabolism, Excretion, and Toxicity.

Entry Name	QPpolrz	QPlogS	QPlogPC16	QPlogPw	QPlogPo/w	QPlogKp	QPlogKhsa
NPC18185	44.271	-2.1	16.269	36.295	-2.452	-7.33	-0.624
NPC98583	65.081	-0.639	24.495	57.852	-5.536	-9.789	-1.811
NPC100251	65.355	-0.174	25.598	64.181	-6.833	-11.062	-1.835
NPC112380	61.805	-0.637	24.609	58.396	-6.621	-11.269	-2.044
NPC171932	43.451	-1.93	15.271	31.285	-1.519	-6.286	-0.596
NPC300657	63.983	-4.051	20.104	35.85	-0.646	-8.053	-0.351
NPC471403	67.624	-3.705	20.691	38.097	-0.23	-7.17	-0.268
NPC471404	65.069	-2.684	20.534	41.03	-1.062	-7.586	-0.306
NPC472454	45.442	-2.048	17.118	39.549	-3.12	-8.014	-0.728
NPC473010	62.142	-4.62	18.407	27.791	1.687	-5.949	0.193

Molecular Dynamic (MD) simulation

MD simulation is a computational assessment for the stability and dynamics of the ligand-receptor complex under physiological conditions. In this study, MD simulation was performed to access the stability of all ligand-NDM-1 docked complex and their docking poses. Fifty ns of molecular dynamics simulations were applied for all complexes. Backbone RMSD and RMSF of each complex's trajectory with respect to their initial conformation showed the stability of the complex. The average and standard deviation of backbone RMSD during the last ten ns were shown in Table 4. The small standard deviations indicated that all protein structures reach to stable structures during the last 10 ns of MD simulation.

Table 4
The average of backbone RMSD of proteins during the last 10 ns of MD simulation (only the last three digit of name of compounds were mentioned).

	PRO	NPC185	NPC 251	NPC 380	NPC 403	NPC 404
Back-bone RMSD (nm)	1.53 ± 0.015	1.52 ± 0.01	1.41 ± 0.007	1.22 ± 0.027	1.33 ± 0.012	1.15 ± 0.006
	NPC 454	**NPC 583**	**NPC 657**	**NPC 932**	**NPC 3010**	
Back-bone RMSD (nm)	1.48 ± 0.009	1.22 ± 0.009	1.42 ± 0.011	1.39 ± 0.007	1.67 ± 0.015	

Therefore, it can be inferred NPs could make a stable complex with NDM-1 and inhibit NDM-1 protein.

Figure 4 *RMSD analyses of ten natural compounds in complex with NMD-1. (only the last three digit of name of compounds were mentioned).*

Figure 5. *RMSF analyses of all complexes during the last 10 ns of MD simulation.*

Table 5 exhibits the value of the MM-PBSA and MM-GBSA binding free energy of every ligand to its protein and also thermodynamics parameters of all complexes. All NPs showed a high binding affinity for NDM-1. Among the compounds, NPC472454 had the lowest binding energy)-137.12 kcal/mol (. Thermodynamic parameters with a negative value of the ΔH and ΔG exhibited the event possibility of the binding between proteins and ligands was exothermic. These results confirm RMSD and RMSF results.

Table 5
Thermodynamic parameters of binding ligands to NDM

complex	$\Delta G_{MM-PBSA}$ (kcal/mol)	$\Delta G_{MM-GBSA}$ (kcal/mol)	ΔS (kcal/mol)	ΔH (kcal/mol)
NDM1-NPC18185	-49.82	-48.23	-77.11	-23037.18
NDM1-NPC98583	-49.99	-53.92	-110.85	-33079.04
NDM1-NPC100251	-54.45	-57.43	-78.81	-23551.65
NDM1-NPC112380	-53.76	-49.24	-99.56	-29737.57
NDM1-NPC171932	-55.54	-58.12	-79.60	-23788.28
NDM1-NPC471403	-32.07	-33.80	-96.80	-28892.92
NDM1-NPC471404	-43.11	-39.01	-94.86	-28135.89
NDM1-NPC472454	-137.12	-136.83	-74.40	-22319.48
NDM1-NPC473010	-75.84	-74.40	-92.56	-27672.60
NDM1-NPC300657	-56.75	-54.99	-87.53	-26213.44

3D conformational alignment and pharmacophore modeling

In this step, crucial conserve residue in all metallo-β-lactamase classes was identified (Table S2)

Comparisons of 3D conformational alignment, protein sequence alignment over 700 subtype of MBL, pharmacophore, distance and angles displayed that these properties among the crucial residues of metallo-β-lactamase classes were similar (Fig S8, S9 and S10)

Discussion

Global contamination of NDM-1 has become a major threat to human health. Currently, there is no NDM-1 clinically inhibitor. The discovery and development of an inhibitor for inhibiting of NDM-1, as well as restituting and reinforcing the efficacy of the beta-lactam antibiotic against this enzyme would have a significant effect on human health and create obvious socio-economic benefits [25]. These limitations and uttermost necessity inspired us to mine a new lead compound against NDM-1 from natural resources [26].

The reconnaissance of novel non-covalent inhibitors of β-lactamases is an optimistic path to preserve and restore the efficacy of β-lactam antibiotics.

Against this study, different and frequent studies have investigated some chelator compounds of the zinc of NDM and MBL (26, 28), but some studies indicated that mutation in non-active site residues sequences over some MBLs could severely decrease the dependency of these enzymes on zinc ions, therefore, concentrating on the metal's chelators are not proper option. Even in the starvation of zinc and utilization of EDTA as a metal chelator, MBLs was powerful enough to degrade beta-lactam rings [27–29].

Other studies examined the compounds affecting one type of the MBL subclasses alone. During those studies, no effort was made to find common pharmacophore and crucial residues playing a key role in the active site (residues conserved in the active site of all kinds of MBL) in all MBL classes [25]. In this study, regarding the above-mentioned weakness, the crucial conserved residues (hotspots residues) playing a key role in the active site and common pharmacophore in all MBLs were detected.

Hotspots of the active site were recognized by our post-docking analyses and were mentioned by others [30, 31]. Hotspots of amino acids that could be employed more effectively with configured lead molecules against the binding site of NDM-1 were Ser217, Ser251, Asn220, Asp124, His250, Lys211, Ile35. Among them, Ile35 involved in the Van der Waals interactions to all complexes. Also, His189, Gly219, Asp124 and His122 significantly contributed to the hydrophobic interactions alongside Ile35. These amino acids played an essential role in stabilizing the complex via hydrogen bonds or hydrophobic contacts. Alignment on all types of NDM (NDM-1 - NDM30 Figure S4) showed that all the above-considered amino acids not only played a pivotal role in binding with the active site, but also conserved in all types of NDM. Therefore, they can be used for the pharmacophore modeling and ligand discovery in future studies.

Our precise 3D conformational alignment over the tertiary structure of all metallo-β-lactamases and BLDB database alignment on the second structure of these proteins proved that the above amino acids conserved in all metallo-β-lactamases (most likely play a role in the catalysis reaction in the active site). Ser251, Asn220, Asp124, His250, His189, Gly219 and His122 residues conserved in the B1 and B2 subclass and for all three subclasses Asp124, His250, His189 and His122 conserved. Hence there is a possibility for our ten natural compounds in binding with all MBL subclasses and inhibiting them (because of interaction with these residues)

The discussed ligands based on these common pharmacophores and key residues may inhibit all MBLs. It would be cost-benefit effective in drug design and can inhibit broad types of the enzymes.

An insight into NDM-1 structures showed that a water molecule situated between Zn 302 and Zn 303, performs as a nucleophile during hydrolysis of the β-lactam ring of antibiotics. Analyses of the hydrolysis process by NDM indicated that prominent part served by the aforementioned residues in maintaining the overall structure and function of NDM-1.

The NPASS database was used as the database, which had a complete collection of 35032 natural compounds. For this purpose, 35032 compounds were screened, and 1300 compounds were docked.

Finally, among them, ten compounds were selected. Since all ten compounds had interactions with those critical residues, there is a possibility to inhibit all types of MBLs, more investigations and laboratory experiments are essential.

Two steps of structural screening were done to found the best ligands with high ability for inhibition of the NDM1. At first, captopril was used in structural screening and NPC120633 ligand was obtained. Then to catch a better ligand with lower binding free energy, second screening based on the similarity to NPC120633 was performed and ten ligands with lower binding energy than NPC120633 were found.

Multi-step molecular docking assisted in facilitating the virtual screening process by yielding insight into the ligand binding energy and docking binding affinity. Multiple molecular docking using the Autodock Vina (module of LigandScout) software and structural screening via the infiniSee software help to identify the best NPs that could perfectly inhibit NDM-1. SeeSAR and Schrödinger suite softwares were applied to confirm secondary virtual screening (secondary docking) results. Schrödinger and SeeSAR results approved the Autodock Vina results for ten final compounds. Validation of docking was confirmed by using Glide XP-docking and Glide SP-docking.

In this study, ten inhibitors had high affinity, and the docking score against NDM-1 and their binding revealed an exothermic pattern for Gibbs free energy and entropy changes. The value of MM-PBSA and MM-GBSA binding free energy was considerable for all compounds and also the results obtained from RMSD and RMSF plots exhibited that all ten compounds made strong and stable complexes with NDM-1. Thus, these compounds can compete with β–lactam antibiotics to bind with NDM-1 and survive them from hydrolyzes by this enzyme. These NPs are suggested as the potential lead to develop future drug candidates.

Conclusion

The initial aim of the present study was to inhibit NDM-1 by natural compounds. Moreover, it was decided to investigate the active site residues and interactions of these amino acids to ligands. It was supposed that if our compounds were selected by this method, they could inhibit most of MBL.

Several 3D conformational alignments were applied on the subclasses of MBLs to find conservatory of the key residues playing a crucial role in the interaction with ligands. Thus, if our natural compounds can interact with these residues, they will possibly inhibit all types of MBLs. 3D alignment, investigation about space location of crucial amino acids in the active site, and pharmacophore modeling can be employed as excellent and comprehensive methods in drug design. Future studies about MBLs can benefit from our results, compounds and protocol to find the potential drug in order to inhibit MBLs.

Our team selected natural products owing to their availability and natural compounds derived from this source were more cost-effective than small molecules. The ten chosen natural compounds can inhibit NDM-1 in computational methods, and based on our study, maybe they inhibit all or most of MBL classes. Among these ten NPs, NPC472454 was the best inhibitor for NDM-1 inhibition and it can be a candidate drug for MDR infections.

Abbreviations

NDM-1; New Delhi metallo-β-lactamase-1, MBL; Metallo-β-lactamases, MDR; Multi drug resistance, RMSD; Root mean square deviation, RMSF; Root mean square fluctuation, NP; Natural product.

Declarations

Competing interests

The authors declare no conflicts of interest.

Availability of data and materials

The authors confirm that the data supporting the findings of this study are available within the manuscript [and/or] its supplementary materials.

Ethics approval and consent to participate

Not applicable, as no human participants, data or tissue or animals are

Funding

This research is an extract from the PhD dissertation (No. 398337) of the Isfahan University of Medical Sciences. The university approved and supported this study. Funding for PhD was from Isfahan University of Medical Sciences.

Authors' contributions

AS, designed and performed the experiments, derived the models and analyzed the data. KM, analyzed the results and generated the figures. PS, generated the models to calculate. MSD, wrote the manuscript with support from AS. JF, supervised the project. All authors read and approved the final manuscript

Acknowledgment

Not applicable.

References

1. Knowles JR (1985) Penicillin resistance: the chemistry of. beta.-lactamase inhibition. Acc Chem Res 18(4):97–104

2. Patel G, Bonomo R (2013) “Stormy waters ahead”: global emergence of carbapenemases. Frontiers in microbiology 4:48
3. Bush K (2010) Alarming β-lactamase-mediated resistance in multidrug-resistant Enterobacteriaceae. Curr Opin Microbiol 13(5):558–564
4. Bush K, Jacoby GA (2010) Updated functional classification of β-lactamases. Antimicrob Agents Chemother 54(3):969–976
5. Yong D, Toleman MA, Giske CG, Cho HS, Sundman K, Lee K, Walsh TR (2009) Characterization of a new metallo-β-lactamase gene, blaNDM-1, and a novel erythromycin esterase gene carried on a unique genetic structure in Klebsiella pneumoniae sequence type 14 from India. Antimicrob Agents Chemother 53(12):5046–5054
6. Groundwater PW, Xu S, Lai F, Váradi L, Tan J, Perry JD, Hibbs DE (2016) New Delhi metallo-β-lactamase-1: structure, inhibitors and detection of producers. Future medicinal chemistry 8(9):993–1012
7. Kumarasamy KK, Toleman MA, Walsh TR, Bagaria J, Butt F, Balakrishnan R, Chaudhary U, Doumith M, Giske CG, Irfan S (2010) Emergence of a new antibiotic resistance mechanism in India, Pakistan, and the UK: a molecular, biological, and epidemiological study. The Lancet infectious diseases 10(9):597–602
8. Shakil S, Azhar E, Tabrez S, Kamal M, Jabir N, Abuzenadah A, Damanhouri G, Alam Q (2011) New Delhi Metallo-β-Lactamase (NDM-1): An Updates. J Chemother 23(5):263–265
9. Nordmann P, Boulanger AE, Poirel L (2012) NDM-4 metallo-β-lactamase with increased carbapenemase activity from Escherichia coli. Antimicrob Agents Chemother 56(4):2184–2186
10. Faheem M, Rehman MT, Danishuddin M, Khan AU (2013) Biochemical characterization of CTX-M-15 from Enterobacter cloacae and designing a novel non-β-lactam-β-lactamase inhibitor. PLoS One 8 (2)
11. Skagseth S, Akhter S, Paulsen MH, Muhammad Z, Lauksund S, Samuelsen Ø, Leiros H-KS, Bayer A (2017) Metallo-β-lactamase inhibitors by bioisosteric replacement: Preparation, activity and binding. Eur J Med Chem 135:159–173
12. Ramana KV, Singhal SS, Reddy AB (2014) Therapeutic potential of natural pharmacological agents in the treatment of human diseases. BioMed research international 2014
13. Dias DA, Urban S, Roessner U (2012) A historical overview of natural products in drug discovery. Metabolites 2(2):303–336
14. Mushtaq S, Abbasi BH, Uzair B, Abbasi R (2018) Natural products as reservoirs of novel therapeutic agents. EXCLI J 17:420
15. Zeng X, Zhang P, He W, Qin C, Chen S, Tao L, Wang Y, Tan Y, Gao D, Wang B (2018) NPASS: natural product activity and species source database for natural product research, discovery and tool development. Nucleic acids research 46(D1):D1217–D1222
16. Dassault Systèmes BIOVIA (2016) Discovery Studio Modeling Environment, Release 2017. Dassault Systèmes, San Diego

17. Wolber G, Langer T (2005) LigandScout: 3-D pharmacophores derived from protein-bound ligands and their use as virtual screening filters. J Chem Inf Model 45(1):160–169
18. Trott O, Olson AJ (2010) AutoDock Vina: improving the speed and accuracy of docking with a new scoring function, efficient optimization, and multithreading. J Comput Chem 31(2):455–461
19. Laskowski RA, Swindells MB (2011) LigPlot+: multiple ligand–protein interaction diagrams for drug discovery. ACS Publications
20. Pandey RK, Kumbhar BV, Sundar S, Kunwar A, Prajapati VK (2017) Structure-based virtual screening, molecular docking, ADMET and molecular simulations to develop benzoxaborole analogs as potential inhibitor against Leishmania donovani trypanothione reductase. Journal of receptors signal transduction 37(1):60–70
21. Lindorff-Larsen K, Piana S, Palmo K, Maragakis P, Klepeis JL, Dror RO, Shaw DE (2010) Improved side-chain torsion potentials for the Amber ff99SB protein force field. Proteins: Struct Funct Bioinf 78(8):1950–1958
22. Da Silva AWS, Vranken WF (2012) ACPYPE-Antechamber python parser interface. BMC Res Notes 5(1):367
23. Salari-Jazi A, Mahnam K, Hejazi SH, Damavandi MS, Sadeghi P, Zeinalian M, Tabesh F, Mirbod SM, Khanahmad H Predicting and repurposing of drug and drug like compounds for inhibition of the covid-19 and its cytokine storm by computational methods
24. Verma P, Tiwari M, Tiwari V (2018) In silico high-throughput virtual screening and molecular dynamics simulation study to identify inhibitor for AdeABC efflux pump of Acinetobacter baumannii. Journal of Biomolecular Structure Dynamics 36(5):1182–1194
25. Linciano P, Cendron L, Gianquinto E, Spyrakis F, Tondi D (2018) Ten years with New Delhi Metallo-β-lactamase-1 (NDM-1): from structural insights to inhibitor design. ACS infectious diseases 5(1):9–34
26. Tang YT, Marshall GR (2011) Virtual screening for lead discovery. In: Drug Design and Discovery. Springer, pp 1–22
27. Cheng Z, Thomas PW, Ju L, Bergstrom A, Mason K, Clayton D, Miller C, Bethel CR, VanPelt J, Tierney DL (2018) Evolution of New Delhi metallo-β-lactamase (NDM) in the clinic: effects of NDM mutations on stability, zinc affinity, and mono-zinc activity. J Biol Chem 293(32):12606–12618
28. Cheng Z, Miller CG, Williams C, Poth R, Morris M, Lahey O, Nix JC, Tierney DL, Page RC, Crowder MW Clinical Variants of New Delhi Metallo-β-Lactamase are Evolving to Overcome Zinc Scarcity. Alexander Robert Bergstrom:110
29. Liu Z, Li J, Wang X, Liu D, Ke Y, Wang Y, Shen J (2018) Corrigendum: Novel Variant of New Delhi Metallo-β-lactamase, NDM-20, in Escherichia coli. Frontiers in microbiology 9:497
30. Zhang H, Hao Q (2011) Crystal structure of NDM-1 reveals a common β-lactam hydrolysis mechanism. FASEB J 25(8):2574–2582
31. Zhang H, Ma G, Zhu Y, Zeng L, Ahmad A, Wang C, Pang B, Fang H, Zhao L, Hao Q (2018) Active-site conformational fluctuations promote the enzymatic activity of NDM-1. Antimicrob Agents Chemother 62(11):e01579–e01518

Figures

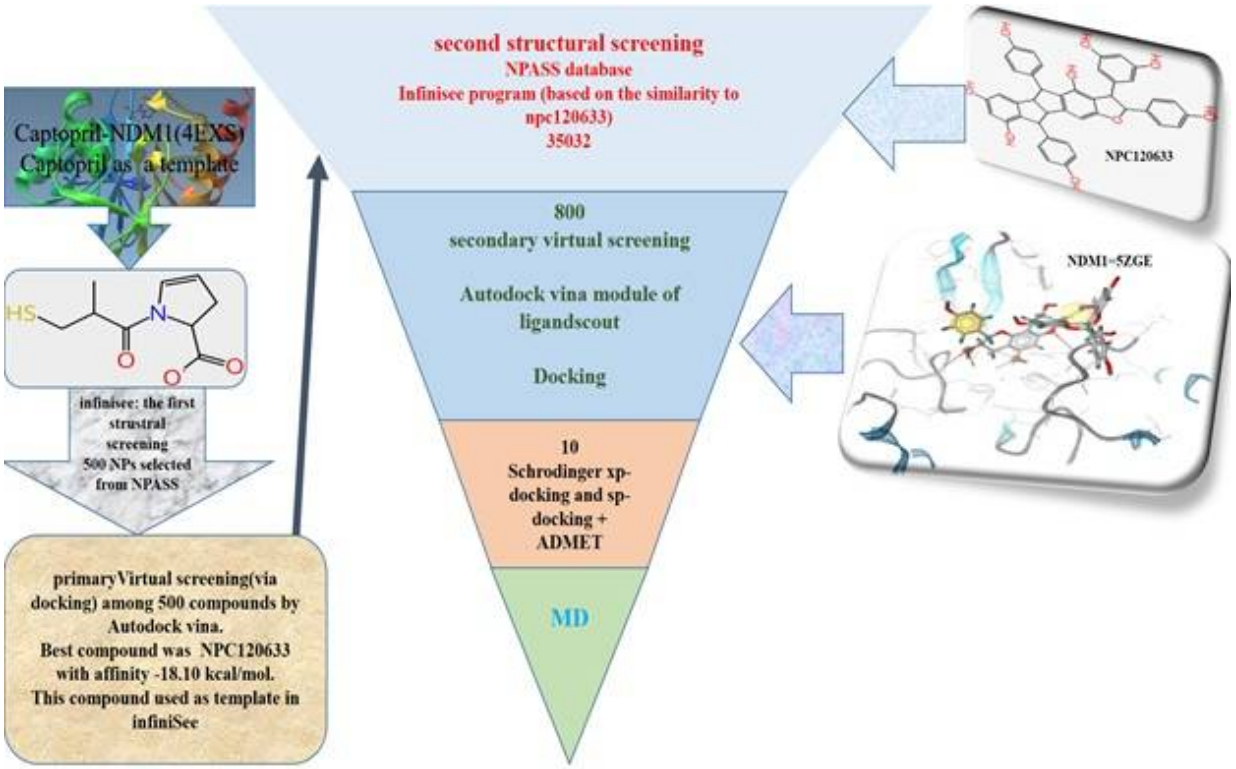

Figure 1

The procedure of this study

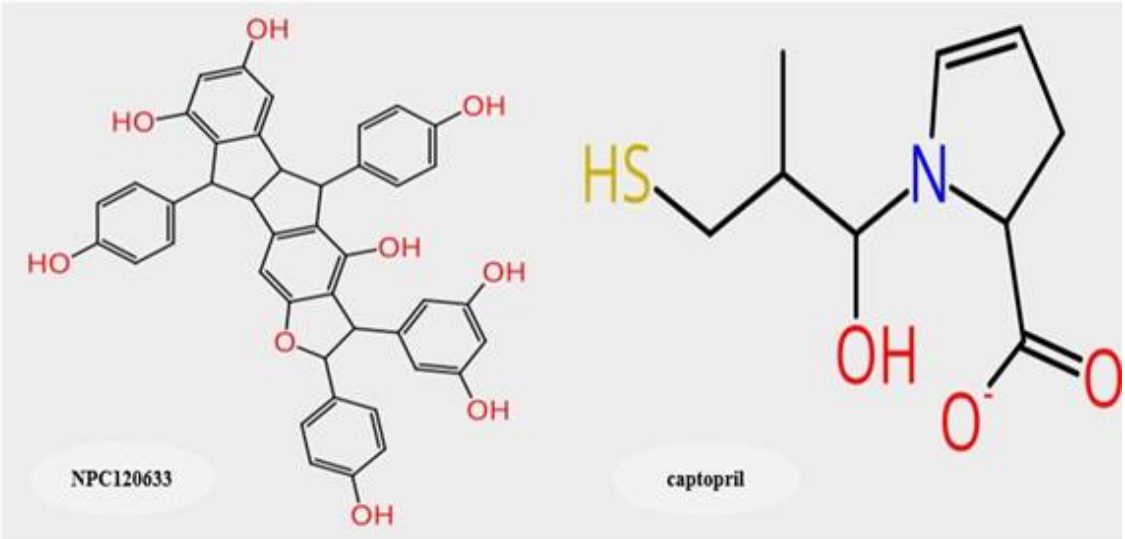

Figure 2

The structure of captopril and NPC120633.

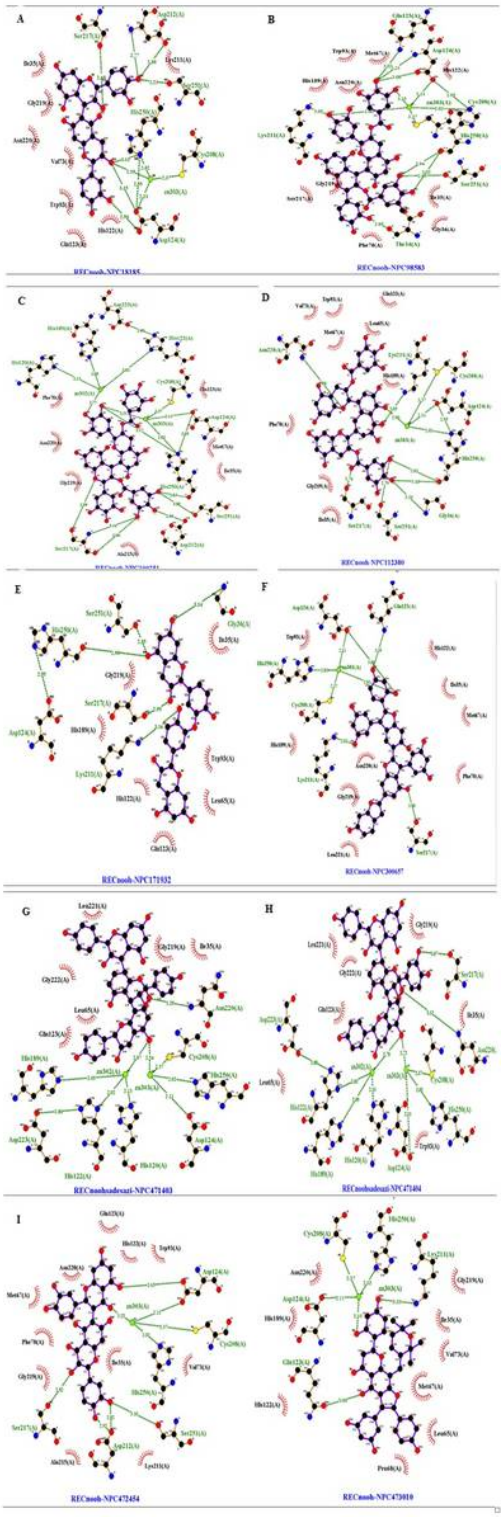

Figure 3

The predicted complex NDM1-NPC binding mode. The position of the NPs in the active site of the NDM1, hydrogen bonds and hydrophobic interactions were shown. A= NDM1-NPC18185, B= NDM1-NPC98583, C= NDM1-NPC100251, D= NDM1-NPC112380, E= NDM1-NPC171932, F= NDM1-NPC300657, G= NDM1-NPC471403, H= NDM1-NPC471404, I= NDM1-NPC472454, J= NDM1-NPC473010

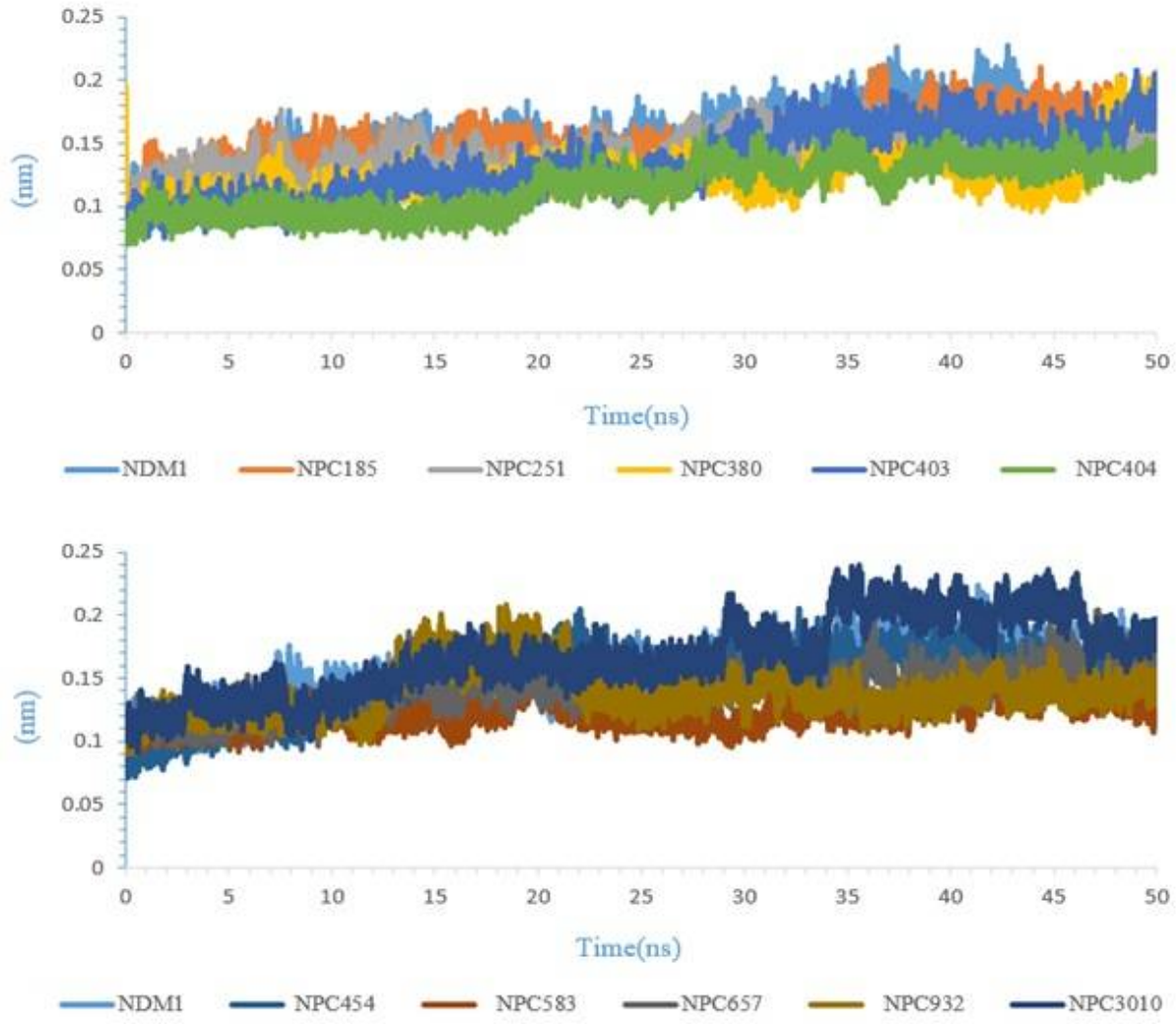

Figure 4

RMSD analyses of ten natural compounds in complex with NMD-1. (only the last three digit of name of compounds were mentioned).

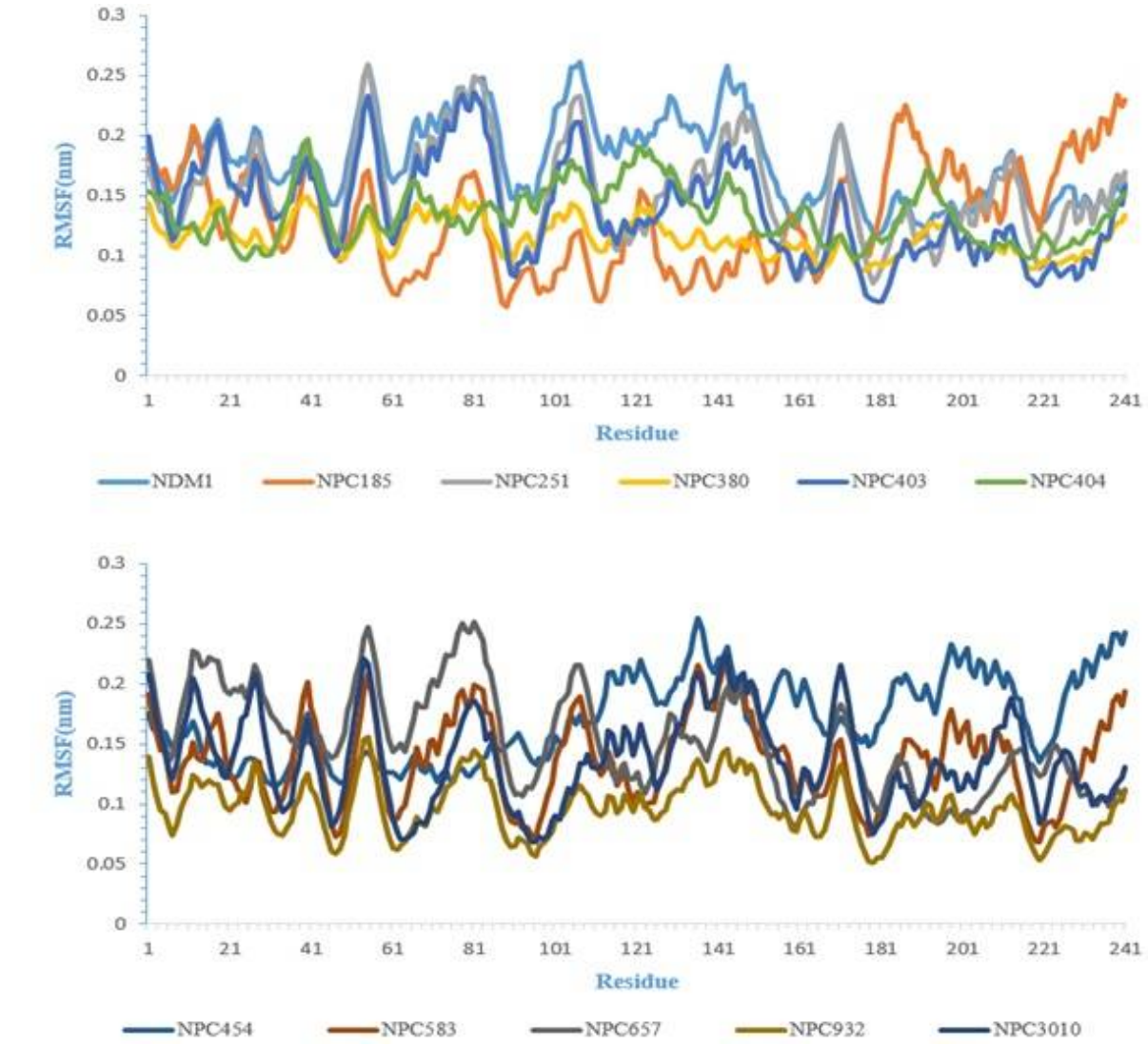

Figure 5

RMSF analyses of all complexes during the last 10 ns of MD simulation.

Supplementary Files

This is a list of supplementary files associated with this preprint. Click to download.

- Graphicalabstract.tif
- SUPLEMNTARY.docx